Published in final edited form as:
Genesis. 2009 September ; 47(9): 579–589. doi:10.1002/dvg.20536.

Cell Adhesive Affinity Does Not Dictate Primitive Endoderm Segregation and Positioning During Murine Embryoid Body Formation

Robert Moore[1], **Kathy Q. Cai**[2], **Diogo O. Escudero**[3], and **Xiang-Xi Xu**[1,3,*]

[1]Department of Medicine, Sylvester Comprehensive Cancer Center, Department of Obstetrics and Gynecology, University of Miami Miller School of Medicine, Miami, Florida 33136

[2]Ovarian Cancer Program, Fox Chase Cancer Center, Philadelphia, Pennsylvania 19111

[3]Graduate Program in Cell and Developmental Biology, University of Miami School of Medicine, Miami, Florida 33136

Summary

The classical cell sorting experiments undertaken by Townes and Holtfreter described the intrinsic propensity of dissociated embryonic cells to self-organize and reconcile into their original embryonic germ layers with characteristic histotypic positioning. Steinberg presented the differential adhesion hypothesis to explain these patterning phenomena. Here, we have reappraised these issues by implementing embryoid bodies to model the patterning of epiblast and primitive endoderm layers. We have used combinations of embryonic stem (ES) cells and their derivatives differentiated by retinoic acid treatment to model epiblast and endoderm cells, and wild-type or *E*-cadherin null cells to represent strongly or weakly adherent cells, respectively. One cell type was fluorescently labeled and reconstituted with another heterotypically to generate chimeric embryoid bodies, and cell sorting was tracked by time-lapse video microscopy and confirmed by immunostaining. When undifferentiated wild-type and *E*-cadherin null ES cells were mixed, the resulting cell aggregates consisted of a core of wild-type cells surrounded by loosely associated *E*-cadherin null cells, consistent with the differential adhesion hypothesis. However, when mixed with undifferentiated ES cells, the differentiated primitive endoderm-like cells sorted to the surface to form a primitive endoderm layer irrespective of cell-adhesive strength, contradicting the differential adhesion hypothesis. We propose that the primitive endoderm cells reach the surface by random movement, and subsequently the cells generate an apical/basal polarity that prevents reentry. Thus, the ability to generate epithelial polarity, rather than adhesive affinity, determines the surface positioning of the primitive endoderm cells.

Keywords

cell segregation; cell sorting; embryos; germinal layers; cell adhesion; epithelial polarity; endoderm; morphogenesis

*Correspondence to: Xiang-Xi Michael Xu, UM/Sylvester Comprehensive Cancer Center, Department of Medicine, University of Miami School of Medicine, Miami, FL 33136. xxu2@med.miami.edu.

Additional Supporting Information may be found in the online version of this article.

INTRODUCTION

How cells, following a few fundamental physical principles, spontaneously sort and assemble into distinct structures and germinal layers in early development continue to intrigue cell and developmental biologists (Foty and Steinberg, 2005; Gumbiner, 2005; Peifer, 1998; Tepass *et al*., 2002). The intrinsic ability of vertebrate early embryonic cells to sort and organize into embryonic germinal cell layers was first demonstrated experimentally in the now classical work of Townes and Holtfreter. They dissociated and isolated cells from germ layers of amphibian gastrulae and showed that the heterotypically mixed cells spontaneously segregated and laminated according to the inside—outside position characteristic of their histological arrangements in the original embryo. Townes and Holtfreter (1955) speculated that the compartmentalization they observed arose from directed cell movements and selective tissue affinities (Steinberg and Gilbert, 2004). In contrast, Steinberg formulated the "differential adhesion hypothesis" to account for this cell-sorting behavior (Steinberg, 1962, 1963). The "differential adhesion hypothesis" is an important mechanism to explain the remarkable ability of cell sorting and pattern formation in early embryos. In essence, the hypothesis states that cell mixtures dynamically explore various configurations so that weaker cell—cell adhesions are progressively displaced by stronger interactions. The net result is a global consolidation of cell adhesion and arrival at the lowest entropically favorable configuration, with cells less avidly bonded concentrically engulfing those more strongly bound (Steinberg, 1962, 1963). This hypothesis is attractive, because it implies that pattern formation is achieved by relatively simple mechanisms, that is, quantitative differences, perhaps minimal, in the expression of a cell-adhesion molecule (Foty and Steinberg, 2005; Steinberg and Gilbert, 2004). The cadherin cell-adhesion molecules are thought to be critical for cell positioning and patterning in embryogenesis, and the differential adhesion hypothesis is generally well accepted both for the interpretation of germinal cell segregation in early embryogenesis (Foty and Steinberg 2005; Gumbiner, 2005; Peifer, 1998; Tepass *et al*., 2002) and in the explanation of the cell sorting experiments performed in 1955 by Townes and Holtfreter (Steinberg and Gilbert, 2004).

Recently, the genesis of the primitive endoderm in preimplantation mouse embryos has been re-examined in more detail (Chazaud *et al*., 2006; Rossant *et al*., 2003; Rula *et al*., 2007). These observations have challenged the established notion of how primitive endoderm is allocated and asymmetrically positioned facing the blastocoel. Differentiation is now speculated to occur within the inner cell mass, from which the nascent primitive endoderm cells sort to the surface to form an epithelium overlaying the inner cell mass (Chazaud *et al*., 2006; Rossant *et al*., 2003; Rula *et al*., 2007), in a manner highly reminiscent to the cell sorting scheme elaborated by Townes and Holtfreter (Townes and Holtfreter, 1955). We have revisited this issue to determine if cell-adhesive affinity is indeed the determining factor in the positioning of primitive endoderm using cell aggregates, referred to as "embryoid bodies," generated from heterotypic mixtures of murine embryonic stem (ES) cells in suspension (Capo-Chichi *et al*., 2005; Coucouvanis and Martin, 1995). In this embryoid body model, ES cells interact, assemble, and metamorphose into spheroids that are subsequently enveloped by a layer of primitive endoderm cells (Capo-Chichi *et al*., 2005; Coucouvanis and Martin, 1995). We used timelapsed video microscopy to track cell sorting in chimeric embryoid bodies composed of wild-type and *E*-cadherin-null ES cells to examine the importance of cell-adhesive affinity in cell sorting during the formation of the primitive endoderm layer.

MATERIALS AND METHODS

Western Blotting and Antibodies

Cells or spheroids were lyzed in 1×SDS—PAGE lysis buffer (0.05M Tris—HCl pH 6.8, 0.1 M DTT, 2% SDS, 10% glycerol, and 0.1% bromophenol blue) and boiled prior loading. SDS

—PAGE was performed using 7.5% polyacrylamide gels. Fractionated proteins were subsequently electrophoretically transferred to Trans-Blot pure nitrocellulose (Bio-Rad) membranes. Primary mouse monoclonal antibodies used in this study were: anti-*E*-cadherin (BD Transduction Labs #610181), anti-Disabled-2 (Dab2) (BD Transduction Labs #610465), anti-*N*-cadherin (BD Transduction Labs #610920), anti-*P*-cadherin (BD Transduction Labs #610227), and anti-β-actin (Sigma #A5441). The secondary antibody was horseradish peroxidase (HRP) conjugated anti-mouse (Zymed). SuperSignal West Extended Duration Substrate (PIERCE) was used for chemoluminescent detection of proteins.

ES Cell Isolation, Propagation, and Differentiation

RW4 and 9j mouse ES cell lines have been described previously (Larue *et al*., 1996; Rula *et al*., 2007). All ES cell lines were perpetuated in a pluripotent state by culture upon irradiated murine embryonic fibroblasts in ES cell media supplemented with 1000 U/ml of recombinant LIF (ESGRO, Chemicon International). GRE15 and CFG37 murine ES cells were generated de novo from blastocysts obtained from mating βACT::eGFP hemizygotes (Okabe *et al*., 1997) with C57BL/6 female mice using a procedure described previously (Moore *et al*., 1999). ES cells were differentiated into endoderm by exposure to 1 μM all trans retinoic acid for 4–7 days as monolayers cultured in gelatin-coated tissue-cultured dishes. All cell cultures were propagated in a 5% CO_2, 95% air humidified incubator.

Transfection and Fluorescence Activated Cell Sorting

ES cells were transiently transfected with a histone H2B-green fluorescent fusion protein (H2B-GFP) construct (Kanda *et al*., 1998) using Lipofectamine 2000 (Invitrogen). GFP-positive cells were selected by FACS performed on a FACSVantage SE system with Diva (digital vantage) software (Becton Dickinson). If the experiment required the transfection of ES cells differentiated by retinoic acid, then the cells were first differentiated and then subsequently transfected and sorted. The stably transfected 9j-GFP ES cells were generated by transfection of 9j ES cells with the H2B-GFP vector and repeated cycles of FACS selection for GFP followed by cell expansion. The final population of 9j-GFP cells stably and evenly expressed H2B-GFP in all cell nuclei.

Cell-Adhesion Assay

The rate of cell adhesion as an indication of cell-adhesive affinity was measured using a Coulter Counter. Cells were monodispersed with trypsin/EDTA and resuspended at a density of 2×10^6/ml in 10-ml ES cell media buffered with 10 mM Hepes, pH 7.4. The resuspended cells were kept at 37°C on a gyratory shaker rotating at 150 rpm. At each time point, an aliquot was analyzed for particle number in triplicate with a Z1 Beckman Coulter Particle Counter. The threshold for particle size was set at 8 μm to account for individual cell (the size of an ES cell is about 15 μm) and cell aggregates. A reduction of particle number over time is an indication of the rate of cell aggregation.

Chimeric Embryoid Body Formation

Heterotypic spheroids were made by inoculating equal numbers of two ES cell types, where one population was GFP-labeled and was either undifferentiated or prior differentiated, *E*-cadherin null, or wild type, in ES cell media including LIF.

Immunohistochemistry and Immunofluorescence of Spheroids/Embryoid Bodies

Spheroids/embryoid bodies were fixed with formalin, paraffin embedded, and sectioned at 5-μm thickness. Slides were deparafinized in a graded ethanol series, washed in water, and boiled in antigen retrieval solution (DakoCytomation). The same primary antibodies used to detect *E*-cadherin and Dab2 on a Western Blot were used for immunohistochemistry and

immunofluorescence. The polyclonal rabbit antibody to megalin was a gift from Dr. Joachim Herz (University of Texas Southwestern). For immunohistochemistry, the secondary antibody was HRP conjugated anti-mouse (DakoCytomation). For immunofluorescence, the sections were permeabilized with 0.5% Triton X-100 for 15 min and washed three times with PBS, blocked with 3% BSA in PBS containing 0.1% Tween-20 for 30 min at room temperature. The cellular localization of the antigens was revealed by AlexaFluor 594-conjugated anti-mouse (red fluorescence) and AlexaFluor 488-conjugated anti-rabbit (green fluorescence) secondary antibodies. The nuclei were stained with 4′-6-diamidino-2-phenylindole (DAPI) solution. The Nikon Eclipse E800 epifluorescence microscope with 60× oil immersion objective linked to a Roper Quantix CCD camera was used for observation and acquisition. Images were merged using Adobe Photoshop.

Laser Confocal Microscopy of Spheroids/Embryoid Bodies

Confocal imaging was performed using Nikon E800 upright microscope with BioRad Radiance 2000 confocal scanhead fitted with a 10× Nikon Plan Fluor objective (numerical aperture of 0.3) and a 488-nm argon laser. Harvested eight-bit images (GFP channel and phase contrast) were processed with LaserSharp2000 software (Bio-Rad). To digitize the three-dimensional topography of GFP positive and negative cells within a spheroid, serial *z*-sections were acquired axially every 5 μm from top to bottom.

Automated Time-Lapse Video-Tracking of Cell Sorting in vitro

Time-lapse video microscopy was used to image the dynamics of cell sorting in situ. ES cells, either pluripotent or prior differentiated, were trypsinized, heterotypically mixed at equal density and allowed to chelate for 4 h on a Fisherbrand bacterial dish in 10 ml of ES cell media at 37°C. These premature amalgamates were then added drop wise to wells of a 12 well plate containing 1 ml of 0.7% (w/v) sodium alginate (Sigma, A2158) dissolved in ES cell media buffered with 10 mM Hepes at pH 7.2. A small volume of mineral oil covered the well to limit evaporation.

Time-lapse image acquisition was performed by serial imaging of up to 80 memorized *xyz* coordinates (“spots,” corresponding to heterotypic cell aggregates) on both green fluorescence channel and phase contrast every hour for up to 72 h using an automated motorized stage. Either a 10× or 20× Nikon Plan Fluor objective lens (N/A = 0.3 for 10×, 0.45 for 20×) were used on an inverted Nikon TE2000 microscope linked to a Cascade 650 (Photometrics) monochrome camera (16-bit images) ran by MetaVue software (Universal Imaging/Molecular Devices). Spots were exposed to light only during image acquisition. All instrumentation were enclosed in a chamber maintained at 37°C. Stacked images were superimposed and concatenated into movies (avi file format) using Metamorph (Universal Imaging/Molecular Devices) imaging software.

RESULTS AND DISCUSSION

E-Cadherin Null ES Cells Are Able to Aggregate into Embryoid Bodies

E-cadherin is the major cell adhesion molecule expressed in early mouse embryos and is necessary for compaction in the formation of blastocysts (Larue *et al*., 1994; Riethmacher *et al*., 1995; Takeichi, 1991). In nascent embryoid bodies from wild-type ES cells, *E*-cadherin was detected on the surface and at cell—cell borders of all cells, and overall the intensity of expression was relatively uniform throughout the entire spheroid (Fig. 1A). Following demarcation of a primitive endoderm layer on the spheroid surface upon further development (Fig. 1B), all cells expressed *E*-cadherin evenly, although those situated in the center of the spheroid appeared to have a slightly greater level (Fig. 1B). Notably, *E*-cadherin was concentrated on the basolateral cell surfaces but was absent from the apical surface of the

primitive endoderm epithelium. The apical membrane was, however, demarcated by the glycoprotein megalin (Fig. 1C,D) (Yang *et al*., 2007). In early stage embryoid bodies prior to the formation of the surface primitive endoderm, primitive endoderm cells (as indicated by positive Dab2 expression) can be found in the interior of some embryoid bodies (Fig. 1E, arrows) (Rula *et al*., 2007). Megalin is expressed in these interior located primitive endoderm cells; however, the megalin protein distributes throughout the cells without sight of a polarized pattern (Fig. 1E, arrows), suggesting that the apical polarity of megalin is established after arrival of the primitive endoderm cells at the surface of the spheroids. These early primitive endoderm cells located in the interior are thought to sort to the surface subsequently (Chazaud *et al*., 2006; Rula *et al*., 2007).

In wild-type ES cells, the overall *E*-cadherin protein level was not altered significantly in either monolayer or spheroids of ES cells with or without differentiation by treatment with retinoic acid (Fig. 2A). Both RW4 (wild type) and 9j (*E*-cadherin null) (Larue *et al*., 1996) ES cells expressed *N*-cadherin (Fig. 2B), the level of which increased in 9j cells treated with retinoic acid. Nevertheless, in undifferentiated RW4 or 9j ES cells *N*-cadherin levels remained the same, suggesting a compensatory response of *N*-cadherin expression by the absence of *E*-cadherin in the differentiated but not undifferentiated cells. Additionally, neither undifferentiated nor differentiated ES cells expressed *P*-cadherin (Fig. 2B).

In comparison, the 9j ES cells, with or without differentiation by retinoic acid treatment, showed morphologies consistent with a much weaker cell—cell adhesion than wild-type RW4 ES cells (Fig. 2C). Additionally, the 9j ES cells in suspension were much slower to nucleate and form embryoid bodies (Fig. 2D). The absence of *E*-cadherin in these spheroids was confirmed by immunostaining (Fig. 2E).

E-Cadherin Null ES Cells Have Reduced Adhesive Affinity but Are Able to Form a Polarized Surface Primitive Endoderm Layer in Embryoid Bodies

To confirm the reduced cell—cell adhesive affinity of *E*-cadherin null cells, we used a Coulter Counter to quantitate the rate of cell aggregation. When dispersed cells were returned to calcium-containing medium to allow cell—cell aggregation, particle number count declined over time, as an indication of the clustering of individual cells to form aggregates (Fig. 3A). Wild-type ES cells are highly adhesive, indicated by rapid decline of particle number overtime, though prior differentiation into endoderm reduced the rate of cell aggregation. The *E*-cadherin null 9j cells, with or without prior differentiation, aggregated slower than the CFG37 wild-type ES cells (Fig. 3A).

The reduced adhesive affinity of 9j compared to wild-type ES cells, either with or without prior differentiation, was obvious (Fig. 3B). Thus, the extent of physical cell—cell contacts was much less in the 9j than the RW4 wild-type ES cells, either with or without differentiation. Although many factors and pathways may potentially regulate properties of cadherins and cell adhesiveness, the deletion of *E*-cadherin dominates cell-adhesive affinity in the current embryoid body system.

The lower levels of *N*-cadherin present in the ES cells presumably mediate the much weaker cell—cell adhesion in *E*-cadherin null ES cells. In fact, we have shown previously that *E*-cadherin null ES cells also differentiate into endoderm and that *E*-cadherin is dispensable for endoderm differentiation and formation of the primitive endoderm epithelium (Rula *et al*., 2007). In the *E*-cadherin null embryoid bodies, endoderm cells as marked by Dab2 staining locate superficially (Fig. 4A). Megalin is distributed on the apical surface (Fig. 4A), indicating *E*-cadherin is dispensable for establishing apical polarity of the endoderm cells. Similar to the embryoid bodies formed from wild-type ES cells, *E*-cadherin null primitive endoderm cells

found in the interior of the embryoid bodies also lack polar distribution of megalin (Fig. 4B, arrow).

Undifferentiated ES Cells Sort into Layers in Chimeric Cell Aggregates According to the Differential Adhesion Hypothesis

Considering the prevalence of *E*-cadherin cell-adhesion molecules in ES cells and embryoid bodies, we designed experiments to determine the importance of cell-adhesive affinity in the arrangement of the two germs layers, the primitive endoderm and ectoderm, emulating the amphibian embryonic cell-sorting experiments (Townes and Holtfreter, 1955). The primitive endoderm is a simple epithelium overlying the pluripotent cells of the inner cell mass that form the epiblast/ectoderm (Beddington and Robertson, 1999; Bielinska *et al*., 1999; Lu *et al*., 2001). The 9j *E*-cadherin-null ES cells were mixed with wild-type ES cells with or without labeling and prior differentiation, and cell-sorting behavior was determined either by confocal microscopy, time lapse video microscopy, or immunohistochemistry. We used either intrinsic GFP-expressing wild-type ES cells (GRE15, CFG37) (Okabe *et al*., 1997) or ES cells labeled by transfection and subsequent FACS purification for the expression of H2B-GFP (Kanda *et al*., 1998). The ES cells, predifferentiated or pluripotent, were then monodispersed, plated at equal density upon a nonadhesive bacterial culture dish, and allowed to coalesce in suspension for 1–3 days. All possible combinations of differentiated and undifferentiated and wild-type and *E*-cadherin-null ES cells were mixed and then analyzed to visualize the topography of GFP-labeled and unlabelled cells within the spheroids. Representative results by confocal microscopy are shown for each combination of the chimeric spheroids/aggregates (see Fig. 5). Examination at low magnification revealed that all combinations of cell types formed spheroids and that nearly all of the spheroids were actually heterotypic (see Fig. 5). We determined that the fluorescent patterns observed indeed reflected bona fide cell distribution without being complicated by potential artifacts such as uneven detection of fluorescence on surface versus in the interior. Overall, the spheroids were generally oval or circular in shape although those composed exclusively of 9j ES cells tended to be the smaller and the most erratically shaped. Spheroid diameter varied considerably in the ranges of 50–250 μm. Cavitation was not observed in these relatively immature embryoid bodies. Whenever pluripotent cells were mixed together homotypically, that is, RW4 and GRE37 (Fig. 5A) or 9j and 9jGFP (Fig. 5G), the resulting spheroids had a random distribution of GFP-labeled and nonlabeled cells, and no biased distribution of GFP-labeled cells in these controls was ever apparent. Notably, as predicted by the differential adhesion hypothesis proposed by Steinberg (1962, 1963), GFP-labeled *E*-cadherin positive cells (CFG37) aggregated mainly in the interior and *E*-cadherin-deficient cells (9j) populated the periphery of spheroids (Fig. 5D).

We also imaged the cell-sorting process as it actually occurred in real time in vitro. In general, most of the cell aggregates selected for examination at time zero eventually accrued into larger multicellular spheroids. Most spheroids remained in suspension and continually moved laterally and even rotated, although a minority adhered to the substrate. Growth in spheroid size was due to both cell proliferation and recruitment of individual or aggregated cells. In all cases, heterotypic aggregates formed in the cultures were composed of cells initially randomly juxtaposed, but the mixtures spontaneously self assembled and progressively the cells acquired their matured and stable distribution, either central or peripheral.

Differentiated ES Cells Sort to Surface Disregarding Their Adhesive Affinity

In experiments mixing differentiated and undifferentiated cells simulating the sorting of embryonic germ layers, differentiated cells sorted to surface to form a primitive endoderm layer, similar to the previous observation (Rula *et al*., 2007). Differentiated RW4 (wild type) cells were externally positioned to undifferentiated CFG37 (wild type, GFP-labeled) cells in spheroids composed of both cell types (Fig. 5B). Likewise, differentiated CFG37 or 9j cells

located superficially when mixed with undifferentiated RW4 or CFG37 cells (Fig. 5C,F). However, a disagreement with the differential adhesion hypothesis was observed when undifferentiated *E*-cadherin null 9j were mixed with the retinoic acid-differentiated wild-type cells (Fig. 5E). In these spheroids, the *E*-cadherin positive primitive endoderm-like cells formed a surface layer that enclosed the *E*-cadherin null ES cells.

We continued our analysis to compare the relative importance of cell-adhesive affinity versus the cell differentiation in the formation of the primitive endoderm layer (Fig. 6A). The unique sorting behaviors of mixtures of highly and lower adhesive ES cells with or without prior differentiation were imaged by time lapse video microscopy. When undifferentiated ES cells were mixed, they sorted unequivocally according to the differential adhesion hypothesis; the wild-type GRE15 or CFG37 ES cells characteristically clustered centrally and were surrounded by a halo of 9j ES cells (Fig. 6B, and movie S1). When 9j *E*-cadherin null ES cells were mixed with prior differentiated GRE15 ES cells (Fig. 6C, movie S2), the differentiated GRE15 cells did not adopt a centric location and were predominantly peripherally located. Spheroids generated from this cell combination were generally smaller, possibly due to the slow formation of the core from *E*-cadherin null ES cells. Apparently, differentiation completely altered the sorting and positioning behavior of the ES cells.

The chimeric spheroids/embryoid bodies were subjected to further analysis by confocal microscopy at a higher magnification. Individual spheroids were imaged by confocal microscopy to visualize the three-dimensional distribution of fluorescent cells (Fig. 6D,E). As predicted by the differential adhesion hypothesis proposed by Steinberg (Steinberg, 1962, 1963), labeled *E*-cadherin positive cells (RW4GFP) aggregated mainly in the interior and *E*-cadherin-deficient cells (9j) populated mainly the periphery of spheroids (Fig. 6D). Of the 30 spheroids from three independent cell-mixing experiments analyzed, a general cell distribution according to the status of *E*-cadherin expression abided, although the pattern of distribution exhibited some imperfections. We interpret these deviations from an ideal pattern of distribution as the “noise” caused by the continuously active and dynamic movement of cells within the spheroids (movie file S1 and S2, Supporting Information).

However, consistent with our observations from time lapse imaging, a disagreement with the differential adhesion hypothesis was observed when undifferentiated *E*-cadherin null 9j were mixed with the retinoic acid-differentiated wild-type RW4GFP cells (Fig. 6E). In these spheroids, the *E*-cadherin positive primitive endoderm-like cells formed a surface layer that enclosed the *E*-cadherin null ES cells. The superficial position of strongly adhesive cells, engulfing the weakly adherent cells, did not comply with the arrangement predicted by the differential adhesion hypothesis (Fig. 6F).

Spheroids generated from the mixing of *E*-cadherin positive and null cells were subjected to histological analysis (see Fig. 7). As anticipated, the formation of an outer primitive endoderm layer, indicated by Dab2-positive staining (Capo-chichi *et al*., 2005), was observed in the majority of spheroids. The peripheral cells were consistently positive, and the cores of the spheroid were negative for *E*-cadherin staining (Fig. 7A). Interestingly, although the Dab2-positive cells were generally restricted to the outer most layer of the spheroids, *E*-cadherin-positive cells included the outer layer and often two to three additional contacting cell layers beneath, as shown by a representative spheroid in a higher magnification (arrow in Fig. 7B). These *E*-cadherin-positive but Dab2-negative cells presumably originated from the fraction of the wild-type RW4 that remained undifferentiated. Thus, the differentiated, *E*-cadherin-positive cells were able to overcome the positioning of the undifferentiated, *E*-cadherin-positive cells that are otherwise centric favored, through their higher adhesive affinity and position them peripherally (Fig. 7C).

CONCLUSION

In summary, when both undifferentiated wild-type and *E*-cadherin null ES cells are mixed, the strongly adherent wild-type cells localize centrally and the more weakly adherent 9j cells peripherally, as predicted by the differential adhesion hypothesis. However, we conclude that although the principle for cell layer distribution according to the differential adhesion hypothesis may be true in many instances, it cannot be applied to the patterning of mouse primitive endoderm layer, as analyzed here using murine embryoid bodies as models. Whether the same mechanism we have found in mammalian cells can be applied to the amphibian embryonic cells experimented with by Townes and Holtfreter (1955) remains to be verified. Rather, the surface positioning of murine primitive endoderm cells enclosing undifferentiated cells is underscored by the autonomous properties of the primitive endoderm cells to assume a surface territory, disregarding relative cell-adhesive affinity of the cell types. One striking characteristic of epithelial cells is their apical-basal polarity, where apical and basolateral membranes have distinct lipid and protein composition (for example see Fig. 1C,D), a phenomenon that is commensurate with primitive endoderm differentiation (Drubin and Nelson, 1996; Yang *et al.*, 2007; Wodarz, 2002). In a previous study, we showed that deletion of Dab2, an endocytic cargo adaptor protein functions in directional endocytic trafficking to establish cellular polarity, is sufficient to compromise surface positioning of extraembryonic endoderm cells in early mouse embryos (Yang *et al*., 2007). We propose that primitive endoderm cell movement during sorting is random and does not depend on ability of the cell to generate polarity. However, once reaching the surface, the formation of an apical polarity and a nonadhesive apical cell surface domain retain surface positioning of the primitive endoderm cells (Yang *et al*., 2007). Once a primitive endoderm cell establishes polarity and creates a nonadhesive apical surface, this is sufficient to anchor the cell superficially and establish a coherent epithelial compartment irrespective of cell adhesive affinity. We speculate that surface affiliation by apical-basal polarity may be a more suitable concept than the differential adhesion to offer a realistic explanation for the organization of epithelial cells enclosing stromal mesenchyme cells.

Supplementary Material

Refer to Web version on PubMed Central for supplementary material.

ACKNOWLEDGMENTS

We acknowledge the skillful technical assistance of Jennifer Smedberg, Malgorzata Rula, Cory Staub, and secretarial help from Patricia Bateman. We appreciate the contributions of Cass Renner and Fangping Chen of the Histopathology Facility, Dr. Sandra Jablonski for help with confocal and time-lapse video microscopy, and James Oesterling for flow cytometry. We thank our colleagues, Drs. Elizabeth Smith, Ken Zaret, Fabrice Roegiers, for comments, critical review, and editing of this manuscript. We appreciate the gift of the 9j ES cells from Dr. Lionel Larue (Institute Curie, Orsay, France).

Contract grant sponsor: NCI, NIH, Contract grant numbers: R01 CA095071, CA79716 and CA75389

LITERATURE CITED

Beddington RS, Robertson EJ. Axis development and early asymmetry in mammals. Cell 1999;96:195–209. [PubMed: 9988215]

Bielinska M, Narita N, Wilson DB. Distinct roles for visceral endoderm during embryonic mouse development. Int J Dev Biol 1999;43:183–205. [PubMed: 10410899]

Capo-Chichi CD, Rula ME, Smedberg JL, Vanderveer L, Parmacek MS, Morrisey EE, Godwin AK, Xu XX. Perception of differentiation cues by GATA factors in primitive endoderm lineage determination of mouse embryonic stem cells. Dev Biol 2005;286:574–586. [PubMed: 16162334]

Coucouvanis E, Martin GR. Signals for death and survival: A twostep mechanism for cavitation in the vertebrate embryo. Cell 1995;83:279–287. [PubMed: 7585945]

Chazaud C, Yamanaka Y, Pawson T, Rossant J. Early lineage segregation between epiblast and primitive endoderm in mouse blastocysts through the Grb2-MAPK pathway. Dev Cell 2006;10:615–624. [PubMed: 16678776]

Drubin DG, Nelson WJ. Origins of cell polarity. Cell 1996;84:335–344. [PubMed: 8608587]

Foty RA, Steinberg MS. The differential adhesion hypothesis: A direct evaluation. Dev Biol 2005;278:255–263. [PubMed: 15649477]

Gumbiner BM. Regulation of cadherin-mediated adhesion in morphogenesis. Nat Rev Mol Cell Biol 2005;6:622–634. [PubMed: 16025097]

Kanda T, Sullivan KF, Wahl GM. Histone-GFP fusion protein enables sensitive analysis of chromosome dynamics in living mammalian cells. Curr Biol 1998;8:377–385. [PubMed: 9545195]

Larue L, Antos C, Butz S, Huber O, Delmas V, Dominis M, Kemler R. A role for cadherins in tissue formation. Development 1996;122:3185–3194. [PubMed: 8898231]

Larue L, Ohsugi M, Hirchenhain J, Kemler R. *E*-cadherin null mutant embryos fail to form a trophectoderm epithelium. Proc Natl Acad Sci USA 1994;91:8263–8267. [PubMed: 8058792]

Lu CC, Brennan J, Robertson EJ. From fertilization to gastrulation: Axis formation in the mouse embryo. Curr Opin Genet Dev 2001;11:384–392. [PubMed: 11448624]

Moore R, Radice GL, Dominis M, Kemler R. The generation and in vivo differentiation of murine embryonal stem cells genetically null for either *N*-cadherin or *N*- and *P*-cadherin. Int J Dev Biol 1999;43:831–834. [PubMed: 10707907]

Okabe M, Ikawa M, Kominami K, Nakanishi T, Nishimune Y. 'Green mice' as a source of ubiquitous green cells. FEBS Lett 1997;407:313–319. [PubMed: 9175875]

Peifer M. Developmental biology. Birds of a feather flock together. Nature 1998;395:324–335. [PubMed: 9759716]

Riethmacher D, Brinkmann V, Birchmeier C. A targeted mutation in the mouse *E*-cadherin gene results in defective preimplantation development. Proc Natl Acad Sci USA 1995;92:855–859. [PubMed: 7846066]

Rossant J, Chazaud C, Yamanaka Y. Lineage allocation and asymmetries in the early mouse embryo. Philos Trans R Soc Lond B Biol Sci 2003;358:1341–1348. [PubMed: 14511480]

Rula ME, Cai KQ, Moore R, Yang DH, Staub CM, Capo-chichi CD, Howe PH, Smith ER, Xu XX. Cell autonomous sorting and surface positioning in the formation of primitive endoderm in embryoid bodies. Genesis 2007;45:327–338. [PubMed: 17506089]

Steinberg MS. On the mechanism of tissue reconstruction by dissociated cells. I. Population kinetics, differential adhesiveness and the absence of directed migration. Proc Natl Acad Sci USA 1962;48:1577–1582. [PubMed: 13916689]

Steinberg MS. Reconstruction of tissues by dissociated cells. Science 1963;141:401–408. [PubMed: 13983728]

Steinberg MS, Gilbert SF. Townes and Holtfreter (1955): Directed movements and selective adhesion of embryonic amphibian cells. J Exp Zool A Comp Exp Biol 2004;301:701–706.

Takeichi M. Cadherin cell adhesion receptors as a morphogenetic regulator. Science 1991;251:1451–1455. [PubMed: 2006419]

Tepass U, Godt D, Winklbauer R. Cell sorting in animal development: Signalling and adhesive mechanisms in the formation of tissue boundaries. Curr Opin Genet Dev 2002;12:572–582. [PubMed: 12200163]

Townes PL, Holtfreter J. Directed movements and selective adhesion of embryonic amphibian cells. J Exp Zool 1955;128:53–120.

Wodarz A. Establishing cell polarity in development. Nat Cell Biol 2002;4:E39–E44. [PubMed: 11835058]

Yang DH, Cai KQ, Roland IH, Smith ER, Xu XX. Disabled-2 is an epithelial surface positioning gene. J Biol Chem 2007;282:13114–13122. [PubMed: 17339320]

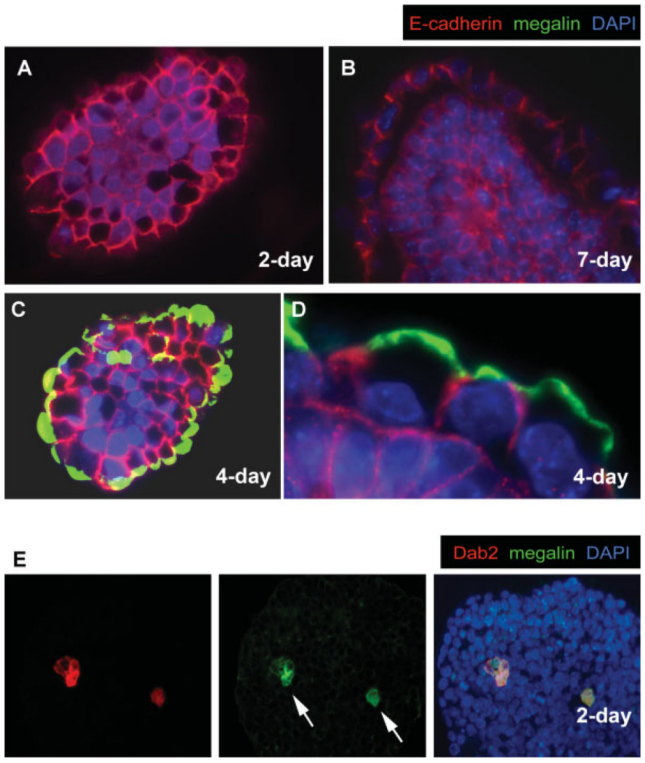

FIG. 1.

Distribution of *E*-cadherin and megalin proteins in embryoid bodies. Embryoid bodies formed from the aggregation of mouse wild-type RW4 ES cells were harvested in various stages, fixed, sectioned, and subjected to immunofluorescence analysis. Merged images of indirect immunofluorescence of *E*-cadherin (red), megalin (green), and nuclei labeled by DAPI (blue) are shown (**A—D**): (A) A representative 2-day-old spheroid prior to the formation of a surface primitive endoderm layer. B: A more mature, 7-day spheroid furnished with a primitive endoderm layer. C: A representative 4-day-old spheroid exhibiting a superficial primitive endoderm layer, and (D) a higher magnification to show the mutually exclusive distribution of megalin and cadherin in surface endoderm cells. Mouse wild-type RW4 ES cells were used to make these spheroids. **E**: A 2-day-old spheroid prior to the formation of a surface primitive endoderm layer contains Dab2 (red)- and megalin (green)-positive primitive endoderm cells (arrows) in the interior of the spheroids. [Color figure can be viewed in the online issue, which is available at www.interscience.wiley.com.]

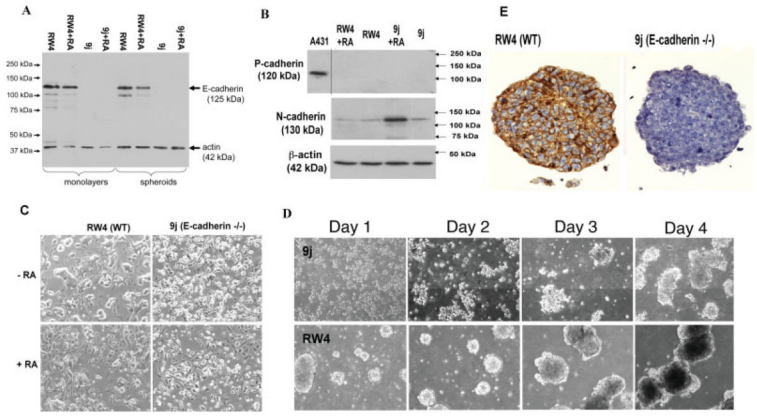

FIG. 2.

Adhesion molecule profiles of *E*-cadherin null ES cells and spheroids. **A**: Quantitative *E*-cadherin expression detected by Western blotting. Wild-type RW4 and 9j *E*-cadherin null ES cells were maintained either as a monolayer or as spheroids with or without retinoic acid for 4 days. The total cell lysate was used for Western blotting simultaneously with both *E*-cadherin and β-actin antibodies. **B**: *N*-cadherin and *P*-cadherin protein levels were analyzed by Western blotting in relation to β-actin levels. A lysate from human A431 cells was included as a positive control for *P*-cadherin. **C**: Cell morphology shown by phase contrast microscopy of RW4 (wild type) or 9j (*E*-cadherin null) ES cells growing as a monolayers with or without 1 μM retinoic acid for 4 days. **D**: Morphology and kinetics of spheroid formation shown by phase contrast microscopy of equal numbers of wild-type RW4 or *E*-cadherin null 9j ES cells in suspension culture for four consecutive days. **E**: Representative *E*-cadherin immunostainings of early spheroids formed by either RW4 wild type or 9j ES cells. [Color figure can be viewed in the online issue, which is available at www.interscience.wiley.com.]

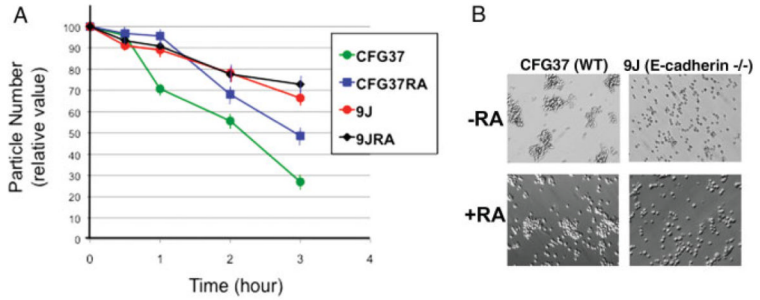

FIG. 3.

Cell adhesion of differentiated and undifferentiated wild-type and *E*-cadherin null ES cells. **A**: Prior differentiated (4 days with retinoic acid) and undifferentiated wild-type and *E*-cadherin null ES cells were assayed for cell adhesion by a reduction of particle number (cells and aggregates) over a 3-h period using a Coulter counter. CFG37, undifferentiated wild-type ES cells; CFG37RA, retinoic acid-differentiated CFG37 ES cells; 9J, *E*-cadherin null ES cells; 9JRA, retinoic acid-differentiated 9J ES cells. The standard error of the mean from the three readings of particle number at each time point of a sample is indicated by an error bar, which is typically smaller than 10%. **B**: Cell morphology shown by phase contrast microscopy of wild type or 9j (*E*-cadherin null) ES cells, with or without prior differentiation with 1 μM retinoic acid for 4 days. The cells were first dispersed as suspension of individual cells using trypsin and EDTA. Then, equal numbers of the cells were suspended in calcium-containing culturing medium and kept in gentle motion in a 37°C incubator for 4 h. Morphology and patterns of cell aggregations were shown by phase contrast microscopy. [Color figure can be viewed in the online issue, which is available at www.interscience.wiley.com.]

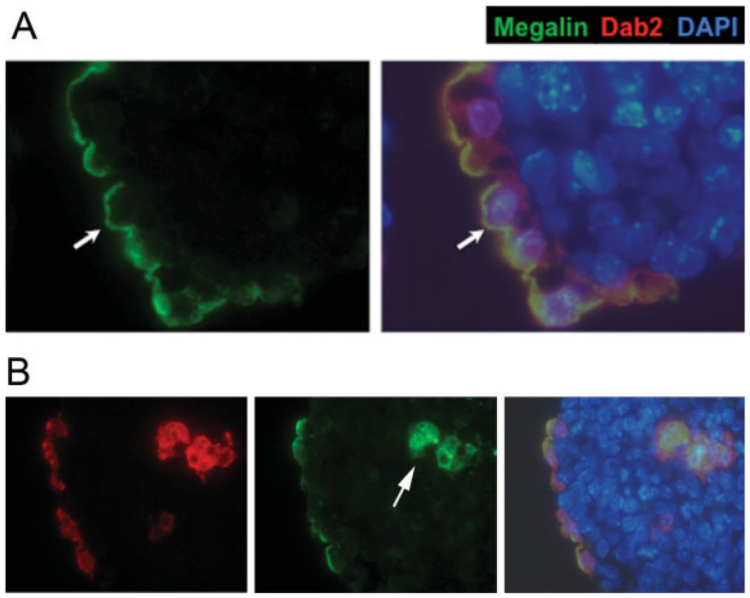

FIG. 4.

Apical polarity of surface endoderm cells in *E*-cadherin null embryoid bodies. **A**: A representative seven-day spheroid produced from the aggregation of 9j *E*-cadherin-null ES cells is shown. The Dab2-positive endoderm cells formed a layer lining the surface and are stained positive for megalin on the apical surface (arrow). Megalin (green) and the merged images of indirect immunofluorescence of Dab2 (red), megalin (green), and nuclei labeled by DAPI (blue) are shown. **B**: An *E*-cadherin (-/-) embryoid body contains Dab2- and megalin-positive primitive endoderm cells located in both the surface layer and the interior (arrow) of the spheroids. Note that megalin is polarized in surface cells but not in the inner cells. [Color figure can be viewed in the online issue, which is available at www.interscience.wiley.com.]

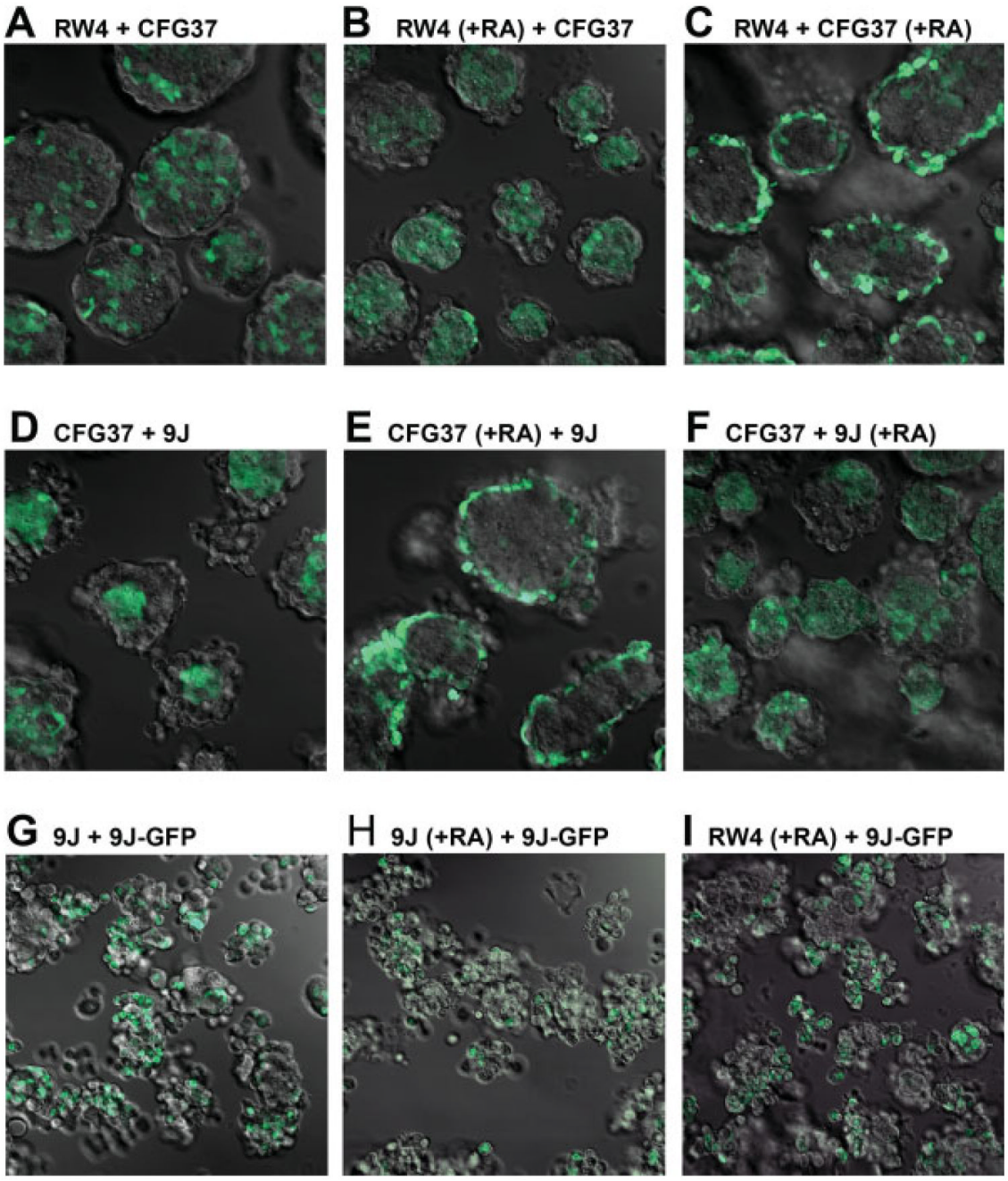

FIG. 5.

Patterns of cell aggregation and sorting in spheroids of various cell composition. Several lines of ES cells including RW4 (wild type), CFG37 (wild type with GFP label), 9j (*E*-cadherin null), and 9j-GFP (9j with GFP label) were used to make 2-day chimeric embryoid bodies. Various combinations of GFP positive and negative cells were mixed in equal number and allowed to form aggregation over a 2-day period. The spheroids formed were imaged for GFP by confocal microscopy. Images of sections near the middle in lower magnification (that allow to see multiple spheroids in one field) were shown. All images were taken at identical magnification and laser power settings. **A**: Spheroids formed from RW4 and CFG37 cells. **B**: Spheroids from retinoic acid-treated RW4 cells and CFG37 cells. **C**: Spheroids from RW4 and

retinoic acid-treated CFG37 cells. **D**: Spheroids formed from CFG37 and 9j cells. **E**: Spheroids formed from retinoic acid-treated CFG37 and 9j cells. **F**: Spheroids formed from CFG37 and retinoic acid-treated 9j cells. **G**: Spheroids formed from 9j and 9j-GFP cells. **H**: Spheroids formed from retinoic acid-treated 9j cells and 9j-GFP cells. **I**: Spheroids formed from retinoic acid-treated RW4 and 9j-GFP cells. Note that the 2-day-old spheroids from 9j and 9j-GFP cells were still loosely packed and not well formed. [Color figure can be viewed in the online issue, which is available at www.interscience.wiley.com.]

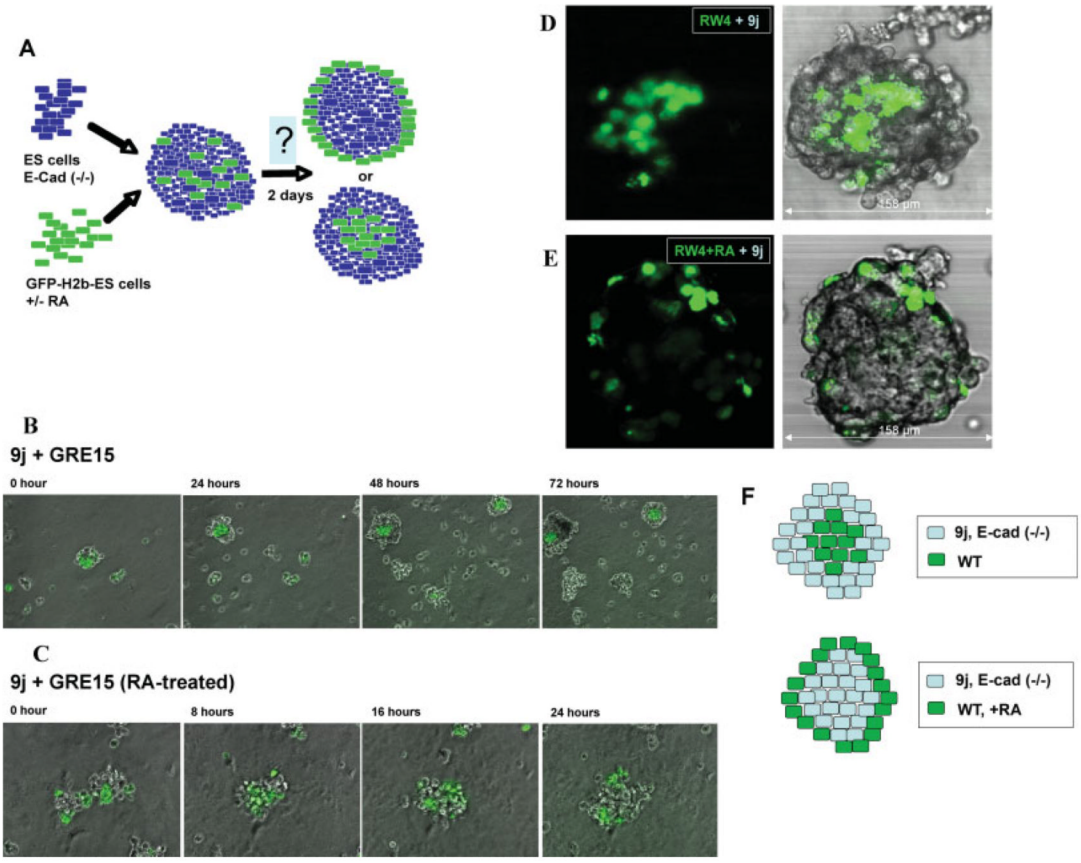

FIG. 6.

Sorting and surface positioning of endoderm cells in spheroids. **A**: Schematic illustration of the cell sorting experimental strategy. ES cells were labeled by transfection with H2B-GFP, and the GFP-expressing cells were collected by flow cytometric sorting. The cells without or with 4 days prior differentiation by retinoic acid-treatment were mixed with unlabeled cells and allowed to form aggregates/embryoid bodies for 2 days. The distribution of GFP-labeled cells was monitored by confocal microscopy. **B, C**: Still images from the time-lapse videos show the patterns of cell sorting after mixing undifferentiated wild-type GRE15 and 9j ES cells (B), and for mixing of retinoic acid differentiated GRE15 and undifferentiated 9j ES cells (C). The respective time-lapse movies are included in the Supporting information. **D**: Results of cell sorting following mixing of undifferentiated GFP-labeled RW4 and 9j ES cells. A representative spheroid was imaged for confocal microscopy sections (35 sections total) from top to bottom to visualize GFP-labeling cells. A middle section (number 17) is shown for both GFP and phase contrast overlay. **E**: Retinoic acid-differentiated GFP-labeled RW4 ES cells were mixed with undifferentiated *E*-cadherin (-/-) 9j ES cells to form aggregates. A representative spheroid was imaged axially (18 sections total) from top to bottom to visualize the GFP-labeled cells. A middle section (number 9) is shown for both GFP and phase contrast overlay. **F**: A caricature illustrates the results of the sorting experiments. When wild types are mixed with *E*-cadherin null ES cells, the wild-type ES cells are sorted to the interior. However, when the wild-type ES cells are first differentiated to endoderm epithelial-like cells, the cells are now peripheral.

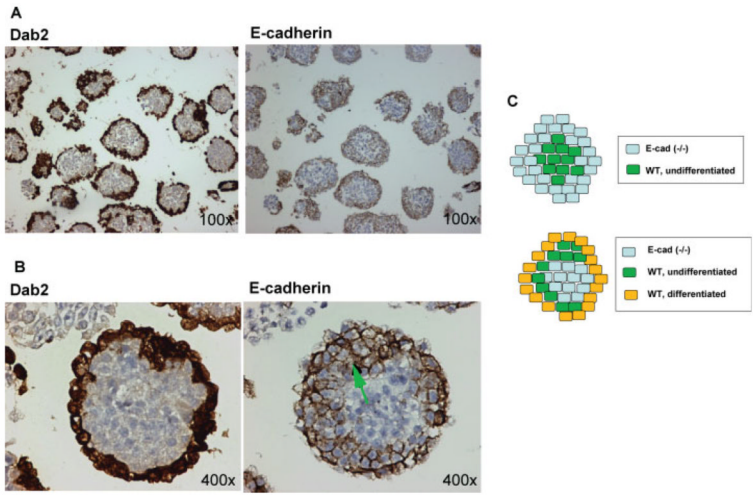

FIG. 7.

Histological analysis of chimeric embryoid bodies. **A**: The 2-day spheroids derived from the mixing of differentiated GFP-labeled RW4 wild-type ES cells with undifferentiated *E*-cadherin (-/-) 9j ES cells were subjected to immunostaining for Dab2 and *E*-cadherin using adjacent sections. **B**: Dab2 and *E*-cadherin immunostaining of a representative spheroid are shown at a higher magnification. The green arrow indicates undifferentiated RW4 ES cells that are Dab2 negative but *E*-cadherin-positive. **C**: Schematic illustration of the results of the sorting experiments. Upper panel, undifferentiated ES cells segregate into a centric core of *E*-cadherin-positive surrounded by *E*-cadherin null cells, according to prediction by the differential adhesion hypothesis. Bottom panel, in spheroids derived from the mixing of differentiated wild type and undifferentiated *E*-cadherin null ES cells, *E*-cadherin-positive endoderm epithelial-like cells form an outer layer on the surface surrounding *E*-cadherin null cells. Following retinoic acid treatment, a small percentage of ES cells remained undifferentiated (strictly saying, not primitive endoderm differentiated). The fraction of these *E*-cadherin-positive but undifferentiated ES cells present in the mixture were segregated between the superficial endoderm and the central *E*-cadherin-null inner cells.